East Eur. J. Phys. Vol.3 No.3 (2016) 92-100

PACS: 52.55.Hc, 52.55.Fa, 07.55.Ge, 52.20.Dq, 91.25.Fd, 75.50.Bb

ABOUT THE VALUES OF THE STRAY ENVIRONMENT FIELDS TO TOROIDAL MAGNETIC FIELD RATIO IN THE URAGAN-2M TORSATRON

G.G. Lesnyakov, **A.N. Shapoval**

Institute of Plasma Physics, National Science Center "Kharkiv Institute of Physics and Technology"
1, Akademichna st., 61108, Kharkiv, Ukraine, Tel.: +38(057)335-64-37; Fax +38(057)335-26-64
e-mail: lesn@kipt.kharkov.ua
Received August 31, 2016

The values of stray environment magnetic fields of the Uragan-2M torsatron have been determined using local magnetic sensors, and also, the electron beam injection in the additional toroidal magnetic field (16 coils, making up 60% to 76% of the total toroidal field). In the stationary toroidal magnetic field, the turns of the electron beam have been visualized by scanning the poloidal vacuum chamber cross-section with a luminescent rod. The measurements have made it possible to determine a decrease in the ratio of stray environment vertical magnetic fields to toroidal-coil magnetic field down to $\tilde{b}_z/B_T \approx 1\times10^{-3}$ at magnetic fields B_T = 0.0225 - 0.15 T, and also, to estimate the prospect of the ratio decrease to $\tilde{b}_z/B_T \approx 1\times10^{-4}$ as the toroidal magnetic field increases up to $B_T \geq 0.45$ T.
KEYWORDS: stellarator, torsatron, tokamak, magnetometer, electron beam, particle orbits, magnetic surfaces, stray environment magnetic fields, environment magnetism, nonmagnetic stainless steel

ПРО СПІВВІДНОШЕННЯ ВЕЛИЧИН ОТОЧУЮЧИХ ПАРАЗИТНИХ ПОЛІВ ДО ТОРОЇДНОГО МАГНІТНОГО ПОЛЯ В ТОРСАТРОНІ УРАГАН-2М

Г.Г. Лесняков, А.М. Шаповал

Інститут фізики плазми, Національний науковий центр "Харківський фізико-технічний інститут"
61108, Харків, вул. Академічна, 1, Україна

Величини розсіяних паразитних полів оточуючого середовища торсатрона Ураган-2М були визначені локальними магнітними датчиками, а також за допомогою інжекції електронного пучка в додаткове тороїдне магнітне поле (в магнітне поле 16 котушок, які утворюють від 60% до 76% сумарного тороїдного поля). Візуалізація обертів електронного пучка в стаціонарному тороїдному магнітному полі виконувалася скануванням полоїдного поперечного перерізу вакуумної камери за допомогою люмінесцентного стрижня. Виміри дали можливість визначити зменшення співвідношення величин оточуючих паразитних полів до магнітного поля тороїдних котушок до величини $\tilde{b}_z/B_T \approx 1\times10^{-3}$ в магнітних полях B_T = 0,0225 – 0,15 Т, а також оцінити перспективу зменшення співвідношення до $\tilde{b}_z/B_T \approx 1\times10^{-4}$ в міру того, як магнітне поле збільшуватиметься до $B_T \geq 0{,}45$ Т.
КЛЮЧОВІ СЛОВА: стеларатор, торсатрон, токамак, магнітометр, електронний пучок, орбіти частинок, магнітні поверхні, паразитні магнітні поля, магнетизм оточуючого середовища, немагнітна нержавіюча сталь

ОБ ОТНОШЕНИИ ВЕЛИЧИН ПАРАЗИТНЫХ ОКРУЖАЮЩИХ ПОЛЕЙ К ТОРОИДАЛЬНОМУ МАГНИТНОМУ ПОЛЮ В ТОРСАТРОНЕ УРАГАН-2М

Г.Г. Лесняков, А.Н. Шаповал

Институт физики плазмы, Национальный научный центр "Харьковский физико-технический институт"
61108, Харьков, ул. Академическая, 1, Украина

Величины рассеянных паразитных полей окружающей среды торсатрона Ураган-2М определены локальными магнитными датчиками, а также при помощи инжекции электронного пучка в дополнительное тороидальное магнитное поле (в магнитное поле 16 катушек, создающих от 60% до 76% суммарного тороидального поля). Визуализация оборотов электронного пучка в стационарном тороидальном магнитном поле выполнялась сканированием полоидального поперечного сечения вакуумной камеры при помощи люминесцентного стержня. Измерения дали возможность определить уменьшение отношения величин паразитных окружающих полей к магнитному полю тороидальных катушек до $\tilde{b}_z/B_T \approx 1\times10^{-3}$ в магнитных полях B_T = 0,0225 – 0,15 Т, а также, оценить перспективу уменьшения отношения до $\tilde{b}_z/B_T \approx 1\times10^{-4}$ по мере того, как тороидальное магнитное поле увеличивается до $B_T \geq 0{,}45$ Т.
КЛЮЧЕВЫЕ СЛОВА: стелларатор, торсатрон, токамак, магнетометр, электронный пучок, орбиты частиц, магнитные поверхности, паразитные магнитные поля, магнетизм окружающей среды, немагнитная нержавеющая сталь

In toroidal nuclear fusion facilities the stray environment magnetic fields may have an appreciable effect on the quality of magnetic surfaces, e.g., see refs. [1-6]. The value of these fields is determined by many factors such as the assembling accuracy of the magnetic system and magnetization of coil casings, the load-bearing toroidal framework of helical windings, the elements of the toroidal vacuum chamber and diagnostics, under-installation structures, the reinforced concrete floor of the experimental hall, etc.

It is known that the efficiency of the magnetic confinement of plasma is sensitive to relative magnitude of the magnetic field disturbance $\tilde{b}/B$, where $\tilde{b}$ is the toroidally averaged magnetic field disturbance, and B is a toroidal magnetic field, in which the plasma confines. Containing $\tilde{b}/B$ to values low enough would lead to much higher energy confinement times. For example, the studies of [7] pointed out that the confinement time τ in a device with $\tilde{b}/B$ is characterized as $\tau \sim (\tilde{b}/B)^{-2}$. Therefore it is believed that the $\tilde{b}/B$ ratio is one of the qualitative features of the

thermonuclear devices. However, it would be to keep in mind that the stochasticity of magnetic field lines which correlates with $\tilde{b}/B$ is not necessarily catastrophic for the magnetic plasma confinement.

In the present work the values of the stray environment magnetic field in the Uragan-2M torsatron have been measured. When studying, the motion of a low-energy electron beam injected into the toroidal magnetic fields of values ranging from B_T = 0.0225 to B_T = 0.1536 T (the field on the geometric torus axis) the beam trajectories and deflection distances along toroidal transits were determined. On the basis of these data the value of the stray environment magnetic fields-to- toroidal-coil magnetic field ratio (the degree of magnetic disturbance) and its variation were found, and, thus, the evaluation was provided of the quality of an additional toroidal magnetic field and, in the whole, the quality of confinement toroidal magnetic field in the URAGAN-2M torsatron.

DESCRIPTION OF THE TORSATRON AND GENERAL FEATURES OF STRAY ENVIRONMENT FIELDS MEASURED WITH A FLUX-GATE METER SENSOR

The Uragan-2M torsatron with an additional toroidal magnetic field (major torus radius R = 1.7 m, minor vacuum chamber radius a_{vc} = 0.34 m) comprises: a helical winding with l = 2 multipolarity and a number of magnetic field periods m = 4; 16 coils of the additional toroidal magnetic field; 8 coils of compensating- and 4 coils of correcting vertical magnetic field. The multipolarity (in our case, l = 2) denotes the number of independent identical helical windings (helical poles), which are used to generate the helical magnetic field. The helical winding is placed on the surface of load-bearing toroidal framework with the minor radius a_{pc} = 0.395 m. A closed magnetic configuration with the helical winding cannot be made without an additional toroidal magnetic field. The part of the toroidal magnetic field of 16 coils in the total toroidal field of such torsatron can vary between 60% and 76% and it depends on the chosen structure of magnetic surface configuration.

The structure of embedded closed magnetic surfaces can be created in a wide range of operating modes [8-11], which make it possible to vary the average radius of closed magnetic surfaces, the profile of the rotational transformation angle of the magnetic field lines, the magnetic well value, the position of the closed magnetic surfaces relative to the vacuum chamber, and also, to get rid of the island structures at the magnetic surfaces. Each operating mode is characterized by two parameters. The first parameter is the interrelation between helical toroidal magnetic field B_h and the additional toroidal magnetic field B_T, $K_\varphi = B_h/(B_h + B_T)$ = 0.28-0.4, where $(B_h + B_T) = B_0$ is the magnetic field on the geometric torus axis. The second parameter is the average vertical magnetic field $\langle B_z \rangle / B_0$ on the geometric torus axis of the compensating/correcting coils that control the magnetic axis position.

The general arrangement of the toroidal device and experimental equipment is schematically represented in Fig. 1.

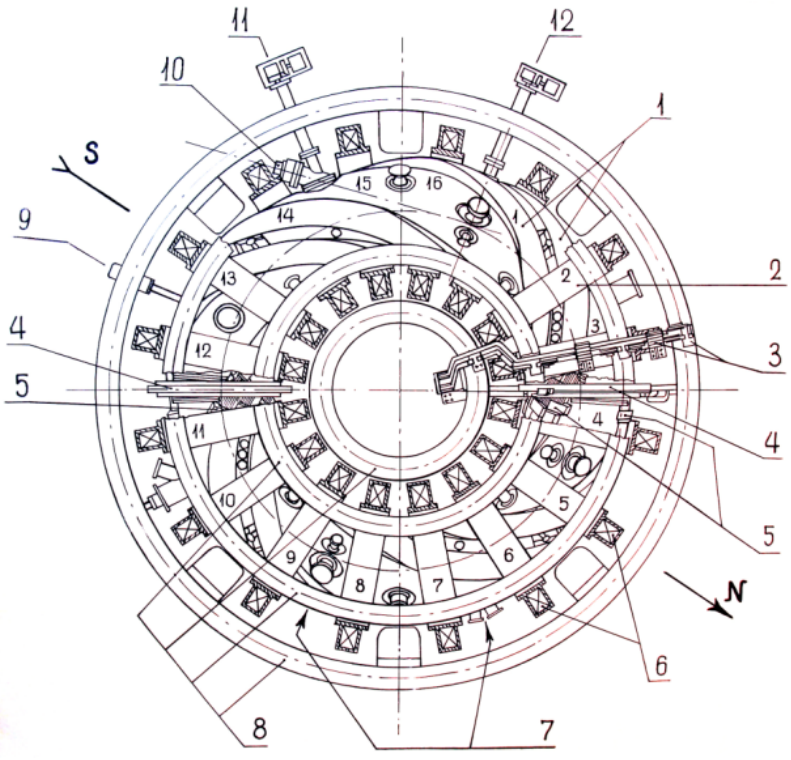

Fig. 1. Schematic of Uragan-2M – top view.

Experimental equipment of the device includes: 1 are the helical windings; 2, 6 are the coils in the casing and in section, respectively (16 toroidal field coils are labeled by small numbers); 3 are the current feeds, 4 are the bandage

fastenings at the separation of the vacuum chamber and the helical winding into two moveable halves; 5 are the detachable joints of helical windings; 7 are the vacuum ports for measuring magnetic surfaces (2007, 2012 and 2014) by the scanning fluorescent rod mounted between coils Nos. 8-9, the butt-end glass to take the image of magnetic surfaces in the tangential direction (to the rod) is situated between coils Nos. 6-7; 8 are the 8 coils of compensating- and 4 coils of correcting vertical magnetic field, 9 is the location of the electron gun during measurements, 10 is the butt-end glass window.

The value of stray environment magnetic fields around the installation is quite readily determined through local measurements using a flux-gate meter sensor placed, for instance, between the toroidal magnetic field coils. Similar measurements have been carried out in 1994 and 2014 on the minor radius, a_c=0.4075 m, nearby the toroidal load-bearing framework of helical windings, Fig. 2.

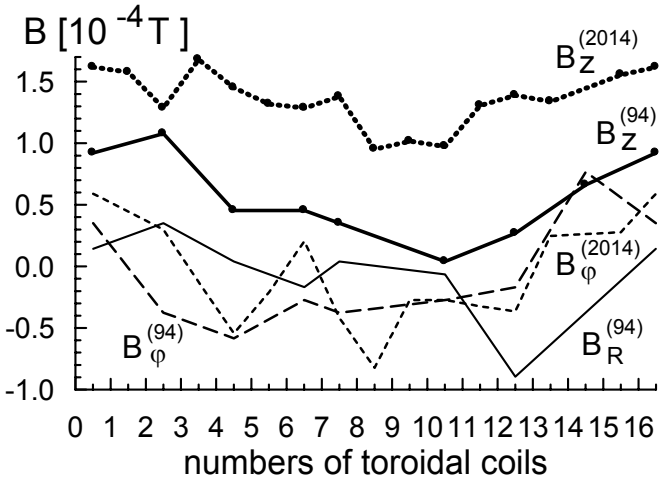

Fig. 2. Changes in the values of stray magnetic field components measured between the coils of the additional toroidal field in the equatorial plane of the Uragan-2M torsatron in 1994 and 2014.

Results of flux-gate meter sensor measurements

The stray magnetic fields were measured in the equatorial torus plane, Fig. 2: B_z is the component parallel to the major torus axis (perpendicular to the torus plane); B_φ and B_R are the tangent and normal components directed to the outer torus circumference. Here, it should be noted that the average value $B_R^{(94)} \approx -0.014\times10^{-4}$ T is very small. It turns out that $B_R^{(2014)} \sim B_R^{(94)}$ and the behavior of these components is very similar. So, not to overload Fig. 2, $B_R^{(2014)}$ is not shown in the figure. The average values of $B_\varphi^{(2014)} \approx -0.057\times10^{-4}$ T and $B_\varphi^{(94)} \approx -0.05\times10^{-4}$ T are close to each other, too. After years of torsatron operation, the value of $B_\varphi^{(2014)}$ changed insignificantly. During measurements, the B_φ value changes its sign when the measurements go clockwise, following the numerical order of the toroidal coils, Fig. 1. At the beginning of the measurements, B_φ shows concordance of signs with the geomagnetic field sign. Then B_φ changes its sign, as it should be in the case of the torus pass-around by. The geomagnetic field direction is shown by S-N in Fig. 1. For the time interval between the above-mentioned years the average value of component B_z has increased by a factor of 2.4; $B_z^{(2014)} \approx 1.354\times10^{-4}$ T and $B_z^{(94)} \approx 0.57\times10^{-4}$ T. The length of stray magnetic field decay in the radial direction from the installation up to the geomagnetic field level ($B_{z(g)}^{(2014)} \approx 0.45\times10^{-4}$ T) is ~ 4.5 m.

The geomagnetic field in the experimental hall both before installation assembly and at the present time has the value ranging from $B_g \approx 0.4\times10^{-4}$ T to $B_g \approx 0.62\times10^{-4}$ T. In the experimental hall under the installation, there is no floor with a reinforcement bar. The principal reinforcement of the installation is located under the device, in the basement, much below the level floor of the experimental hall. Therefore, it is considered that the principal reinforcement and the reinforcement bar floor of the experimental hall practically little affect the stray magnetic fields of the device.

The structure of the toroidal magnetic field coils is according to the project. The accuracy and reliability of their fastening at the assembly of the device, as well as positive results of their power tests in a high toroidal magnetic field are well known for the maintenance Team of the Uragan-2M torsatron and for the authors of the given studies. Therefore, it is difficult for the authors even to surmise the presence of the toroidal coil shape distortion. Besides, additional preventive maintenance and control of the device give no grounds for that surmise.

So, the average value of the vertical stray magnetic field $B_z^{(2014)} \approx 1.354\times10^{-4}$ T is a reference quantity in this study (at $B_T = 0$, $B_0 = 0$, $B_h = 0$, $\langle B_z \rangle = 0$).

It should be noted that all the casings of magnetic system elements and installation components of new devices around the Uragan-2M torsatron are made of nonmagnetic stainless steel 12Cr18Ni10Ti, which has a low magnetic susceptibility [12], ≤3 in relative units. Also, as it has been indicated in paper [12], the magnetic susceptibility of such stainless-steel products, having the welding seams, can increase with their service life, in general, by an order of magnitude. In the LHD [13], the experimental result suggests the existence of another field error source in addition to

the terrestrial magnetism, the influence of which increases with B_T. One of the candidate of the error field is the unsaturated ferromagnetic materials near the machine. Furthermore, the unsaturated ferromagnetic materials near the machine may also contribute to the estimate of the error field, e.g., the magnetic shield for the neutral beam injector and/or diagnostics, stainless steel deteriorated by welding, etc.

MEASUREMENT OF STRAY ENVIRONMENT FIELDS USING THE ELECTRON BEAM

The values of stray environment fields of the installation inside the vacuum chamber were also determined using the electron beam injection into the toroidal magnetic field, B_T (at $B_0 = B_T$, $B_h = 0$, $<B_z>=0$). The magnetic field, B_T, is the field only from 16 coils with an internal radius of their casings $a_c = 0.54$ m. The turns of the e-beam in the stationary toroidal magnetic field were visualized by scanning the poloidal vacuum chamber cross-section with a luminescent rod. The luminescent-rod scanning method [11,13-22] is very convenient and comparatively simple for performing the measurements of this sort. The scanning luminescent rod (pos.7, Fig. 1) was placed between the toroidal field coils Nos. 8-9, where the elliptic magnetic surfaces are vertical. The e-gun moving in the horizontal direction (pos.9, Fig. 1) was installed in the vacuum chamber between coils Nos. 12 and 13 to inject 40 – 50 eV electrons along the magnetic field lines. Previously, the authors have used this method to investigate the magnetic surfaces structure in the Uragan-2M torsatron under the total stationary toroidal magnetic field, $B_0 = 0.1$ T, see e.g. refs. [11,19-22].

The properties of the confining magnetic field are determined, first of all, by the geometry of the magnetic field lines and the character of the $B = |\boldsymbol{B}|$ coordinate dependence. The equation of the magnetic field lines $\frac{dx}{Bx} = \frac{dy}{By} = \frac{dz}{Bz} = \frac{dl}{B}$ can be written as $\frac{d\vec{r}}{dl} = \frac{\vec{B}}{B}$, where dl is the element of the magnetic field line length. Under the action of disturbances, the radii-vectors get the addition. If $\boldsymbol{B} = \boldsymbol{B}_0 + \boldsymbol{b}$, then $\boldsymbol{r} = \boldsymbol{r}_0 + \Delta\mathbf{r}$ and, to a first approximation, taking into account the first-order corrections to the smallness in $\frac{b}{B_0}$, we have $\frac{\Delta\vec{r}}{dl} = \frac{\vec{b}(r_0)}{B_0}$ [ref. 23, page. 52]. If the magnetic field strength B is the local quantity, then the magnetic field lines are the integral characteristics, and they can serve for determination of the average relative field on the magnetic axis.

The axially symmetric vortex-free toroidal magnetic field is an example of the field with closed field lines. When a small, practically arbitrarily directed uniform field is imposed on the toroidal magnetic field, the closed magnetic field lines turn into the spirals moving away from the initial plane [23, page 14]. It is convenient to judge the behavioral pattern of the toroidal field line from the points of intersection of the field line under consideration with an arbitrary poloidal plane of the torus, which is perpendicular to the line direction (i.e., with the torus cross-section φ = const in r, θ, φ coordinates). The cross point is identified as an imaging footprint. If most of the field lines of the toroidal field are closed after one turn along the torus (they have one footprint), then the field lines are the lines of the axially symmetric toroidal field and are annular. However, if the field line does not close on itself, then in the image plane there is a multitude of footprints from a single field line. This trajectory of the field line becomes similar to an open spiral and can cross the torus surface. The multitude of imaging footprints from one field line, which crosses the torus surface, can correspond to the unsymmetrical toroidal field or to the presence of the disturbance fields, which affect the structure of the toroidal magnetic field.

Note, that the measurement procedures using the e-beam, but only for the poloidal harmonics of disturbance fields, have been elaborated at stellarators in [1,2] and applied to several tokamaks [3-6]. In axial torus, the harmonics of the field can suffer toroidal distortions. But, and in this case, too, the registered, non-zero radial displacements of the footprints are caused only by poloidal harmonics, since there exists the zero toroidal harmonic with n=0. By recording the e-beam footprint coordinates after each turn in any of the poloidal torus cross-section, it is possible to determine the geometric characteristics of the field under investigation. In refs. [2,3], the vector deflection field for disturbance fields from the installation structural parts has been first obtained by connecting the initial and end points of each turn of the electron beam. The toroidal e-beam drift (vertical and/or horizontal displacement for one toroidal turn) $\frac{\Delta r(\Delta z,\Delta x)}{2\pi R} = \frac{\tilde{b}}{B_T}$ [1-6] integrally represents the disturbance level allowing us to determine the toroidally averaged disturbance field $\tilde{b}$ and its ratio to the toroidal magnetic field, and to estimate its radial change.

Results for electron beam measurements

From trajectory recordings shown in Fig. 3, one can see that e-beams make 4 to 11 turns and are cut off by the HF antenna installed inside the vacuum volume. It is characteristic that the slope angle of radial displacements of turn footprints θ (radian) = arc tangent($\Delta z/\Delta x$) remains almost unchangeable, $\theta \approx 0.77$ rad, as the beam start points are changing. Using the measured values of Δz and Δx for one turn of beam, it was found that $\tilde{b}_z/B_T = 1\times10^{-3}$ ($\tilde{b}_z = 1.345\times10^{-4}$ T) and $\tilde{b}_x/B_T = 1.1\times10^{-3}$ ($\tilde{b}_R = \tilde{b}_x = 1.49\times10^{-4}$ T). Since the measurements are performed in the toroidal magnetic field, it is more convenient to redefine the poloidal component $\tilde{b}_x$ in the terms of the toroidal component $\tilde{b}_R$. The unchanging slope angle of radial displacements of turn footprints indicates that the field $\tilde{b}_z$ is practically uniform in the toroidal vacuum chamber volume. In this magnetic field we have no way of extracting spatial harmonics from some

other sources of perturbations, e.g., the induced distortion of magnetic coils shapes by the electromagnetic force, or the magnetization of devices installed around the Uragan-2M torsatron. The average slope angle of radial displacements of turn footprints includes the effect of the geomagnetic field. This field can be represented as the stray environment magnetic fields-to-toroidal-coil magnetic field ratio. At B_T = 0.1 T we have B_g/B_T = (4-6)×10^{-4}, but at B_T = 0.5 T the ratio is B_g/B_T = (0.8-1.2)×10^{-4}. Practically, the contribution of the geomagnetic field is always lower than the total value of the stray environment magnetic fields.

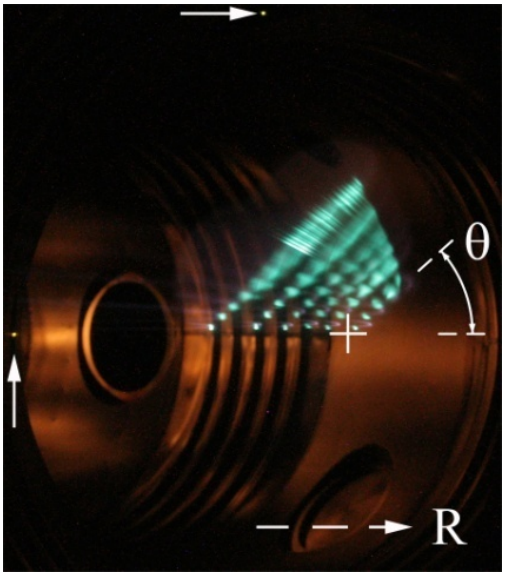

Fig. 3. The e-beam drift footprints in the toroidal magnetic field B_T = 0.1355 T when changing the beam position along R.

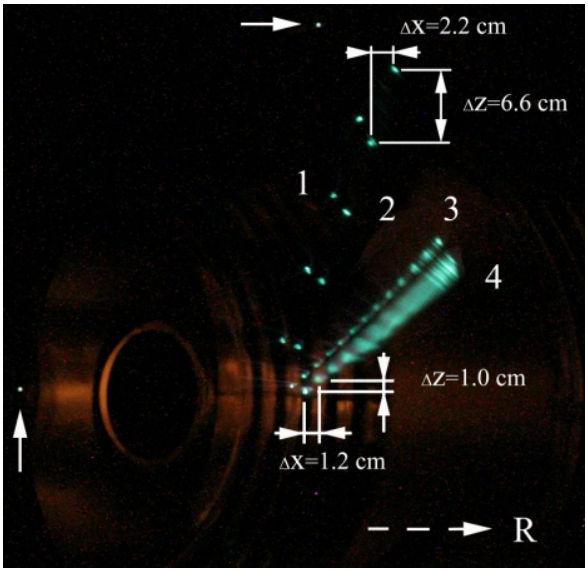

Fig. 4. The e-beam trajectories at different magnetic fields.

Fig. 4 shows how the magnitudes of Δz and Δx are defined. It is essential to note that Fig. 4 also illustrates that the slope angle θ of the beam drift footprint radial displacements in the direction along R in the torus equatorial plane decreases with the toroidal magnetic field increase.

For beam drift trajectories shown in Fig.4 the B_T, $\tilde{b}_z$, $\tilde{b}_z/B_T$, $\tilde{b}_R$, $\tilde{b}_x/B_T$ values were determined, see the Table I.

Table I

The B_T, $\tilde{b}_z$, $\tilde{b}_z/B_T$, $\tilde{b}_R$, $\tilde{b}_x/B_T$ values for beam drift trajectories shown in Fig.4

Beam drift trajectory number	B_T, T	$\tilde{b}_z$,[10^{-4} T]	$\tilde{b}_z/B_T$	$\tilde{b}_R$,[10^{-4} T]	$\tilde{b}_x/B_T$
2	0.0225	1.23-1.39	(5.47-6.2)×10^{-3}	0.394-0.43	(1.75-1.93)×10^{-3}
not shown in the figure	0.0678	1.29-1.43	(1.9-2.11)×10^{-3}	0.92-0.95	(1.36-1.42)×10^{-3}
3	0.1355	1.23-1.56	(0.91-1.15)×10^{-3}	1.32-1.346	(9.8-9.9)×10^{-4}
4	0.1536	1.39-1.6	(0.9-1.05)×10^{-3}	1.6-2.06	(1.05-1.34)×10^{-3}

The e-beam drift trajectories (Fig.4) show that the field lines of the resultant magnetic field look like spirals rotating in the direction of the major radius R increase. The spirals are formed under the action of the magnetic field vector components lying in the poloidal cross-section of the torus. The particularities of the spirals suggest some conclusions about the properties of the poloidal components $\tilde{b}_z$ and $\tilde{b}_R$. The data show (Table I) that $\tilde{b}_z$ weakly grows with B_T increase, and has the values very close to those that were determined with a flux-gate meter sensor. In consequence of magnetization, the component $\tilde{b}_R$ increases more than fourfold with B_T increase. The $\tilde{b}_z/B_T$ and $\tilde{b}_x/B_T$ values show the degree of magnetic disturbance at the toroidal magnetic field B_T. The observed constancy of the spiral slope angle points to constancy of $\tilde{b}_z/\tilde{b}_R$ ratio value. The reduction of spiral trajectories pitch, when B_T increases, it is possible well to see on Fig.4 by comparing the trajectories 2 and 3. The correspondence of ratio $\tilde{b}_x/B_T$ with spiral is determined in Table I. The ratio $\tilde{b}_x/B_T$ defines spiral pitch. Principally, spiral pitch can be determined by the number of e-beam turns along the torus (by the number of spiral turns), which are packed on the length of the minor torus radius. Parallelism of spiral trajectories points to both the homogeneity of $\tilde{b}_z$, and a sufficiently high quality of the toroidal

magnetic field, including its inverse proportionality to the torus major radius (B_T ~ 1/R). In the case under consideration, because of a noticeable difference between the radius of the vacuum camera and the internal radius of the toroidal magnetic field coil casings (a_{vc} = 0.34 m < a_{Tc} = 0.54 m), we can not, unfortunately, register the e-beam drift footprints in the vicinity of the toroidal magnetic field coil casings. As B_T increases and $\tilde{b}_z/B_T$ decreases, the planes of spiral trajectories with small slope angles approach the plane surfaces that are parallel to the torus equatorial plane. With considerable increase in B_T, both $\tilde{b}_z$ and $\tilde{b}_R$ will show the magnetization saturation of the surrounding materials. If $\tilde{b}_z/B_T$ becomes very small and approaches zero with the finite $\tilde{b}_R/B_T$, then, in principle, the spirals can be transformed into the plane spirals (the plane curves), which become parallel to the torus equatorial plane. The behaviour of such spirals (as an example of similar studies) is well substantiated by numerical simulations in the papers [24 (see Appendix A), 25 (see Fig.2c)].

As is seen from the photo the start coordinates of the e-beam originate in the equatorial plane of the torus and move in the direction from the torus geometric axis (marked by +) inwards. The average slope angle for all e-beam drift trajectories is $\theta \approx 0.77$ rad. A smeared image of the e-beam footprints is caused by ~<1% fluctuations of the current in the field coils. The figure also shows two base points from LEDs (indicated by arrows) with the known distance between them. The LEDs were mounted in the measurement section on the inner surface of the vacuum chamber, in the equatorial torus plane on the inner circumference and at the top. The major torus radius is directed from left to right.

The trajectories 1 and 2, marked at Fig.4, were measured at B_T = 0.0225 T (the beams have different starting points and are shown here as examples of the trajectories measured at more favorable conditions than for Fig. 3). The trajectory 2, measured at B_T = 0.0225 T, and the trajectory 3, measured at B_T = 0.1355 T, have one and same starting point of the e-beams. The trajectory 4 was measured at B_T = 0.1536 T. At this field value the starting point of the e-beam was slightly changed because of some technical troubles that caused current fluctuations of the generator energizing the field coils.

Theoretically one can assert that the average angle θ is equivalent to $\tilde{b}_z/\tilde{b}_R$. Using the measured slope angles of the beam drift trajectories, the function θ =f(B_T) plotted in Fig. 5 predicts the saturation magnetization field and the prospect of $\tilde{b}_z/B_T$ decrease as the toroidal magnetic field increases. As regards field $\tilde{b}_R$, a more exact determination of the disturbance and spiral trajectory pitch specified by magnetization field $\tilde{b}_R$ is possible at B_T ~ 0.45 T.

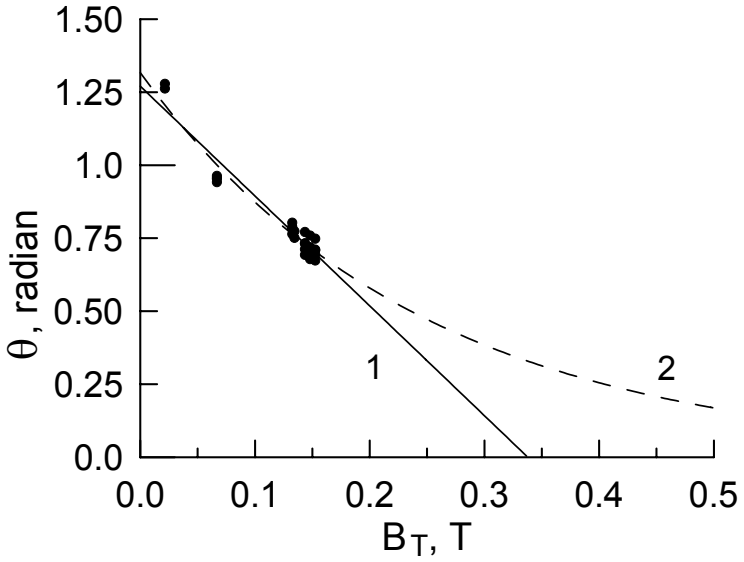

Fig. 5. The average slope angle of the electron beam trajectory θ versus the toroidal magnetic field B_T (experimental data are marked with black points).

In Fig. 5 straight line 1 is a linear extrapolation of the data until it intersects the B_T abscissa and curve 2 is an exponential extrapolation of data in the direction of the B_T abscissa.

The magnetic surfaces measurements in the Uragan-2M torsatron [9,11,19-22] have shown that the main resonances of rotational transform angles and magnetic islands with $i/2\pi$ = 2/7, 1/3, 3/8, 2/5, 1/2, 4/9, 4/7, 4/6, 4/5 result from both the helical winding detachments and the geometry of compensation-field coils. The indicated resonances have been determined numerically and experimentally [9-11, 19, 21-22, 26-33]. The numerical calculations of the magnetic surfaces were performed using the code [26, 27], which describes the current geometry of all torsatron coils in accordance with the design documentation of the device. In the code, special care was given to the simulation of detachable joints of the helical windings [27-29]. The results of comparison between experimental and numerically determined structures of the magnetic surfaces for many operating modes in the region with k_φ = 0.28-0.38 are presented in refs. [8-11, 19, 21, 22, 26-33]. The field disturbances caused by the resonances are significant, and exceed the disturbances that can be induced by the additional toroidal magnetic field and the stray environment fields.

Therefore, in this paper we present both the magnetic surface at the edge and the full structure of closed magnetic surfaces at two modes of configuration settings. At these modes, there are no islands of the above-mentioned resonances, and hence, no other disturbances, except those, which pertain to the purposes of the given investigation. The operating modes of the torsatron require the current powering of all the coils, which form the magnetic configuration. For the indicated modes, the magnetic field values of all torsatron coils are given in the descriptions of Fig. 6,7. It should be also noted that the Uragan-2M torsatron has a generally acceptable level of stray environment fields, since at $B_0 = 0.1$ T high-quality closed magnetic surfaces have been measured, see Fig. 6,7.

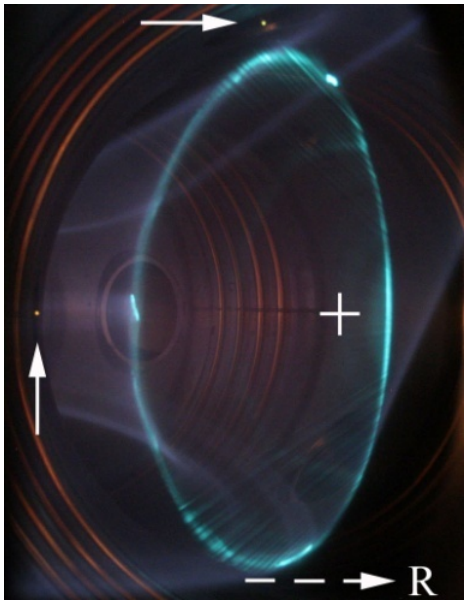

Fig. 6. The last closed magnetic surface with an average minor radius $a = 0.2$ m

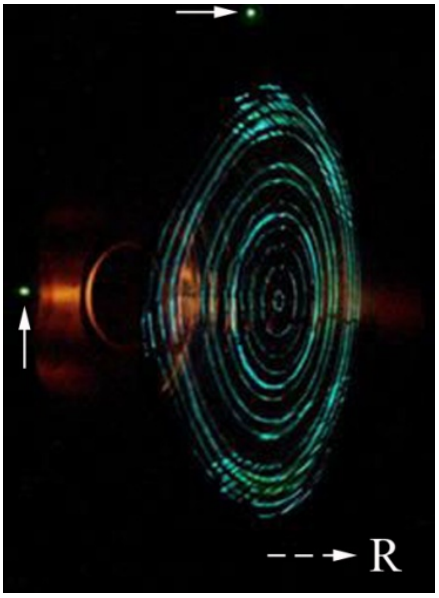

Fig. 7. The structure of the closed magnetic surfaces without magnetic island in the Uragan-2M torsatron

This mode of the magnetic configuration in the Uragan-2M torsatron (Fig.6) has the operating parameter $K_\varphi = 0.31$, and $B_0 = 0.1$ T (where $B_T = 0.0691$ T and $B_h = 0.0309$ T), $(\langle B_z \rangle + \tilde{b}_z)/B_0 \approx 1.85\%$, $i/2\pi(0) \approx 0.32$ and $i/2\pi(a) \approx 0.415$, the shift of the magnetic axis inward from the torus geometric axis (marked by +) is 5.7 cm.

As example, on fig.7 is shown the mode of the magnetic configuration with $K_\varphi = 0.295$, $B_0 = 0.1$ T (where $B_T = 0.0705$ T and $B_h = 0.0295$ T), $(\langle B_z \rangle + \tilde{b}_z)/B_0 \approx 1.8\%$, the average radius of the last closed magnetic surface $a \approx 0.166$ m, $i/2\pi(0) \approx 0.31$ and $i/2\pi(a) \approx 0.4$, displacement of the magnetic axis inward from the geometrical axis of the torus is 4.7 cm.

CONCLUSIONS

The results of local measurements with the use of a flux-gate meter sensor have shown that over the course of 20 years the average vertical component of stray environment fields has increased by a factor of 2.4, and near the load-bearing toroidal framework of the helical winding amounts $B_z^{(2014)} \approx 1.354\times10^{-4}$ T. The stray environment field measurements carried out with an electron beam around the geometric axis of the toroidal vacuum chamber have given $\tilde{b}_z$ to range from 1.23×10^{-4} T to 1.6×10^{-4} T. Comparison shows that the stray environment fields measured by the two methods have very close values.

For the fields with $B_T = 0.1$-0.15 T the value of the stray environment field-to-toroidal-coil magnetic field ratio in the Uragan-2M torsatron is $\tilde{b}_z/B_T \approx 1\times10^{-3}$. For the magnetic fields with B_T between 0.0225 T and 0.1536 T, the increase of the $\tilde{b}_R$ component of stray environment fields from 0.4×10^{-4} T up to $1.6\div2.06\times10^{-4}$ T was observed. This increase being most probably due to magnetization of welding seams in the coil casings. In spite of the fact that the field $\tilde{b}_R$ grows, ratios $\tilde{b}_z/B_T$ and $\tilde{b}_x/B_T$ turn out to be close in values, e.g., at $B_T = 0.1536$ T. According to the measurement data the ratio $\tilde{b}_z/B_T$ decreases and, probably, will be reduced, as extrapolation shows, by an order of magnitude to $\tilde{b}_z/B_T \approx 1\times10^{-4}$, as the toroidal magnetic field increases up to $B_T \geq 0.45$ T.

The measured stray environment field values, which have changed with increase in the operating field, point to a sufficiently high quality of the coil assembly for an additional toroidal magnetic field, and explain the constancy of the slope angle of the e-beam drift trajectories.

In addition, the present studies call attention researchers of similar subject, like study of magnetization of the Uragan-2M elements made from nonmagnetic stainless steel, such as casings of toroidal and compensating field coils, the load-bearing toroidal framework of helical windings, the toroidal vacuum chamber and diagnostics, over a long period of their operation in high magnetic fields. Out of the mentioned elements forming the torsatron, we identify only

the coils for an additional magnetic field as a strong source of the magnetic disturbance, since they have larger (geometrical) dimensions and significant stainless steel mass, long-length weld seams of the casings, and they are located in immediate proximity to the toroidal vacuum chamber.

It has been shown that with the increase in the toroidal magnetic field B_T, a steady decrease of $\tilde{b}_z/B_T$, $\tilde{b}_R/B_T$ and the slope angle of e-beam drift trajectories, can serve as evidence of the reduction of the magnetic disturbances in the device.

Summation the stray uniform vertical field of the magnetization $\tilde{b}_z$ and the field of magnetization $\tilde{b}_R$ to the vertical magnetic field from 8 compensating coils $<B_z>$ does not cause noticeable disturbances of the Uragan-2M torsatron magnetic configuration.

ACKNOWLEDGEMENT

The authors thank Dr. V.S. Voitsenya for the fruitful discussion and critical reading of the manuscript.

REFERENCES

1. Popryadukhin A.P. Behavior of stellarator closed magnetic field lines in the presence of disturbances // Zh. Tekh. Fiz. [Sov. Phys. Tech. Phys.]. – 1964. – Vol.34. – No.4.-P.658-665 (in Russian).
2. Voronov G.S., Popryadukhin A.P. Experimental study of the disturbance effect on the helical magnetic field // Zh. Tekh. Fiz. [Sov. Phys. Tech. Phys.]. – 1964. – Vol.34. – No.10. – P.1786-1789 (in Russian).
3. Mal'tsev S.G., Popryadukhin A.P. Magnetic measurements in the tokamak with TO-2 divertor // Fiz. Plazmy [Sov. J. Plasma Phys.]. – 1988. – Vol.14. – No.7. – P.801-806 (in Russian).
4. Al'khimovich V.A., Akhtyrskii S.V., Babaev I.V., Belikov M.M., Berezovskii E.L., Bondarchuk E.N., et al. Physics Results of the Start up of the T-15 installation // Voprosy Atomnoj Nauki I Tekh. Ser.: Thermonucl. Fusion. – 1998. – Iss. 3. – P.3-17. (in Russian)
5. Neubauer F.H., Bohn F.H., Chudnovskij A., Giesen B., Heuttemann P., Lochter M. // ANS Fusion Technol. – 1997. – Vol.31.– P.154-158.
6. England A.C., Yoon S.W., Kim W.C., Lee D.K., Chung J., Lee K.D., et al. Tokamak field error measurements with an electron beam in KSTAR // Fusion Eng. Design. – 2011. – Vol.86. – P.20-26.
7. Firpo M.-C. Microtearing turbulence: Magnetic braiding and disruption limit // Physics of Plasmas. – 2015. Vol.22. – 122511; http://dx.doi.org/10.1063/1.4938273.
8. Bykov V. E., Georgievskij A. V., Demchenko V. V., Kuznetsov Yu. K., Litvinenko Yu. A., Longinov A. V., Pavlichenko O. S., Rudakov V. A., Stepanov K. N., Tolok V. T. URAGAN-2M: a torsatron with an additional toroidal field // Fusion Technology. – 1990. – Vol.17. – P.140-147.
9. Pavlichenko O. S. for the U-2M group. First results from the "URAGAN-2M" torsatron // Plasma Phys. Control. Fusion. – 1993. – Vol.35. – P.B223-B230.
10. Pavlichenko O. S. Status of "URAGAN-3M" and "URAGAN-2M" experiments // Stellarators and other helical confinement systems, 10-14 May 1993, Garching, Germany. A Collection of Papers Presented at the IAEA Technical Committee Meeting, IAEA, Vienna. – 1993. – P.60-77.
11. Lesnyakov G.G., Pogozhev D.P., Kuznetsov Yu.K., et al. Studies of magnetic surfaces in the "Uragan-2M" torsatron // 23th EPS Conf. on Control. Fusion and Plasma Phys. (Kiev, 24-28 June, 1996). Contributed Papers, EPS. – 1996. – Vol.20C. – Part II, b025. – P.547-550.
12. Azhazha V.M., Desnenko V.A., Ozhigov L.S., Azhazha Zh.S., Svechkarev I.V., Fedorchenko A.V. Using magnetic methods for investigations on the austenitic stainless steel structure evolution after long operation in the NPP power units // Probl. of Atomic Sci. and Technol. Ser.: Phys. Radiation Damages and Radiation Mater. Sci.-2009. (94). NCS KPTI, Kharkiv, Ukraine. – No.4-2. – P.241-246 (in Russian)
13. Morisaki T., Shoji M., Masuzaki S., Sakakibara S., Yamada H., Komori A., Motojima O. and the LHD experimental group. Flux surface mapping in LHD // Proceedings of ITC/ISHW. – 2007.
14. Hailer H., Massing J., Schuler F., et al. Studies the magnetic surfaces in the stellarator Wega // 14 EPS Conf. on Contr. Fusion and Plasma Phys. Madrid, 1987. Contributed Papers. – 1987. – 11 D. – Part I. – P.423-426.
15. Tou T.Y., Blackwell B.D., Sharp L.E. Magnetic field mapping using an image-intensifying fluorescent probe // Rev. Sci. Instrum. – 1991. – Vol.62. – P.1149-1156.
16. Lesnyakov G.G., Volkov E.D., Georgievskij A.V., et al. Study of the magnetic configuration of l=3 torsatron by the triode and the luminescent rod methods // Nuclear Fusion. – 1992. – Vol.32. – P.2157-2176.
17. Jaenicke R., Ascasibar E., Grigull P., et al. Detailed investigation of the vacuum magnetic sufaces on the W7-AS stellarator // Nuclear Fusion. – 1993. – Vol.33. – P.687-704.
18. Shats M.G., Rudakov D.L., Blackwell B.D., et al. Experimental investigation of the magnetic structure in the H-1 heliac // Nuclear Fusion. – 1994. – Vol.34. – P.1653-1661.
19. Tereshin V.I., Beletskii A.A., Berezhnyj V.L., et al. First results of the renewed URAGAN-2M torsatron // 35th EPS Conf. on Plasma Phys (Hersonissos, 9-13 June 2008), ECA. – 2008. – Vol.32. – P.1.061.
20. Gubarev S.P., Ermakov E.B., Lesnyakov G.G., et al. Measuring-controlling complex for investigating the magnetic surfaces of torsatron "Uragan-2M" // Probl. of Atomic Sci. and Technol. Ser.: Plasma Phys. (15), NCS KPTI, Kharkiv, Ukraine. – 2009. – No.1 (59). – P.177-179.
21. Lesnyakov G.G., Shapoval A.N., Pavlichenko O.S. Feasibility of creating an island divertor in the Uragan-2M torsatron // Probl. of Atomic Sci. and Technol. Ser.: "Plasma Phys.", Issue 18, NSC KPTI, Kharkov, Ukraine. – 2012. – No.6(82). – P.34-37.
22. Lesnyakov G.G., Shapoval A.N., Gubarev S.P., et al. Magnetic surfaces of stellarator-mirror hybrid in the Uragan-2M torsatron // Probl. of Atomic Sci. and Technol. Ser.: "Plasma Phys.", Issue 19. NSC KPTI, Kharkov, Ukraine. – 2013. – No.1.(83). –

P.57-60.
23. Morozov. A.I., Solovyov L.S. Geometry of the magnetic field // Voprosy teorii plasmy. – M.: Gosatomizdat, 1963. – Vol.2. - P.3-91.
24. Kotenko V.G. A special correcting winding for the *l*=2 torsatron with split-type helical coils // Fusion Eng. Design. – 2012. – Vol.87. – P.118-123.
25. Kotenko V.G. A special correcting winding for the *l*=2 torsatron with internal splitting of helical coils // Probl. of Atomic Sci. and Technol. Ser.: Plasma Phys. Issue 19, NCS KPTI, Kharkov, Ukraine. – 2013. – No.1(83). – P.24-26; http://vant.kipt.kharkov.ua.
26. Besedin N.T., Kuznetsov Yu.K., Pankratov I.M. The influence of the helical conductor packing on a magnetic configuration of an *l*=2 torsatron with longitudinal field // Voprosy Atom. Nauki i Tekhn., Ser. Termoyad. Sintez, Moskva (Problem of Atomic science and Technique, Ser. Thermonucl. Fusion, Moscow). – 1987. – No.3. – P.18-20. (in Russian)
27. Besedin N.T., Lesnyakov G.G., Pankratov I.M. Currentfeed and detachable joint influence on magnetic field configuration of the Uragan-2M torsatron // Voprosy Atom. Nauki i Tekhn., Ser. Termoyad. Sintez, Moskva (Problem of Atomic science and Technique, Ser. Thermonucl. Fusion, Moscow). – 1991. – No.1. – P.48-50. (in Russian)
28. Besedin N.T., Lesnyakov G.G., Pankratov I.M. Detachable joint and currentfeed influence on the Uragan-4 magnetic configuration // VIII Stellarator Workshop, 27-31 May 1991, Kharkov, USSR. A Collection of Papers Presented at the IAEA Technical Committee Meeting, IAEA, Vienna. – 1991. – P.89-92.
29. Besedin N.T., Lesnyakov G.G., Pankratov I.M. Helical winding detachable joint and currentfeed influence on the Uragan-4 magnetic configuration at the rotational transform less than 0.5 // Stellarators and other helical confinement systems, 10-14 May 1993, Garching, Germany. A Collection of Papers Presented at the IAEA Technical Committee Meeting, IAEA, Vienna. – 1993. – P.477-479.
30. Besedin N.T., Lesnyakov G.G., Pankratov I.M.. Improvement of l=2 torsatron configuration with additional toroidal field // 18th Europ. Conf. on Control. Fusion and Plasma Phys., Berlin.-1991.-Contributed papers. – V15C. – Part.2. – B10.-II-145-II-148.
31. Bykov V.E., Shishkin A.A., Kiβlinger J., Rau F. On vacuum field properties of the Uragan-2M torsatron standard configuration // Preprint IPP 2/301. Garching, FRG.-1989.
32. Zolotukhin A.V., Shishkin A.A. Magnetic island suppression in torsatron // VIII Stellarator Workshop, 27-31 May 1991, Kharkov, USSR. A Collection of Papers Presented at the IAEA Technical Committee Meeting, IAEA, Vienna. – 1991.-IV-P-2.-93-96.
33. Beletskii A.A., Berezhnyj V.L., Burchenko P.Ya. et al. First results of the renewed URAGAN-2M torsatron. // Problem of Atomic Science and Technology (Питання Атомної Науки і Техніки). NCS KPTI, Kharkiv, Ukraine. – 2008. – No.6.(58). – Series: Plasma Physics (14). – P.13-15.